# Strong interactions, narrow bands, and dominant spin-orbit coupling in Mott insulating quadruple perovskite $CaCo_3V_4O_{12}$

H. B. Rhee and W. E. Pickett
*Department of Physics, University of California Davis, Davis, California 95616, USA*
(Received 22 August 2014; revised manuscript received 30 October 2014; published 13 November 2014)

We investigate the electronic and magnetic structures and the character and direction of spin and orbital moments of the recently synthesized quadruple perovskite compound $CaCo_3V_4O_{12}$ using a selection of methods from density functional theory. Implementing the generalized gradient approximation and the Hubbard $U$ correction (GGA + $U$), ferromagnetic spin alignment leads to half-metallicity rather than the observed narrow gap insulating behavior. Including spin-orbit coupling (SOC) leaves a Mott insulating spectrum but with a negligible gap. SOC is crucial for the Mott insulating character of the V $d^1$ ion, breaking the $d_{m=\pm1}$ degeneracy and also giving a substantial orbital moment. Evidence is obtained of the large orbital moments on Co that have been inferred from the measured susceptibility. Switching to the orbital polarization (OP) functional, GGA+OP+SOC also displays clear tendencies toward very large orbital moments but in its own distinctive manner. In both approaches, application of SOC, which requires specification of the direction of the spin, introduces large differences in the orbital moments of the three Co ions in the primitive cell. We study a fictitious but simpler cousin compound $Ca_3CoV_4O_{12}$ (Ca replacing two of the Co atoms) to probe in a more transparent fashion the interplay of spin and orbital degrees of freedom with the local environment of the planar $CoO_4$ units. The observation is made that the underlying mechanisms seem to be local to a $CoO_4$ plaquette, and that there is very strong coupling of the size of the orbital moment to the spin direction. These facts strongly suggest noncollinear spins, not only on Co but on the V sublattice as well.

DOI: 10.1103/PhysRevB.90.205119 PACS number(s): 71.27.+a, 75.25.Dk, 71.70.Ej

## I. INTRODUCTION

Recently, the Mott insulating quadruple perovskite $CaCo_3V_4O_{12}$ (CCVO) was reported by Ovsyannikov *et al.* [1] having been synthesized under pressure. Several other quadruple perovskites with the formula $AA'_3B_4O_{12}$ have been studied, and this class of compounds with two magnetic sublattices has been found to exhibit a wide range of intriguing phenomena, suggesting that its unusual structure may be playing a crucial role in the complex behavior that emerges. $CaCu_3Mn_4O_{12}$ (CCMO) gained attention for its colossal magnetoresistance (CMR) [2], and thus it was compared to the manganates $Ln_{1-x}D_xMnO_3$ (Ln = lanthanide, $D$ = alkali earth metal), which also exhibit CMR. Unlike the structurally simpler manganates, whose magnetoresistance (MR) becomes negligible at low applied magnetic fields, CCMO has a large low-field MR response spanning a wide temperature range below a high ferrimagnetic transition temperature $T_c = 355$ K, a characteristic that is very attractive for magnetic sensor applications. CCMO was found to possess no Jahn-Teller $Mn^{3+}$ ions at the $B$ site and hence no double-exchange mechanism, which is what gives rise to CMR in the manganate perovskites. The origin of CMR (40%) in CCMO, and very large low-field MR in $BiCu_3Mn_4O_{12}$ (Ref. [3]) and $LaCu_3Mn_4O_{12}$ (Ref. [4]) as well, appears to be due to spin tunneling or scattering at grain boundaries, rather than double exchange in the bulk.

Another extreme property was found in the antiferromagnetic insulator $CaCu_3Ti_4O_{12}$, which displays a giant dielectric constant $\sim 10^5$ that remains fairly constant from 100 to 500 K (Refs. [5,6]). This dielectric response was established to be extrinsic in nature, with the structure perhaps playing a central role in the defects that produce very large polarization. Unusual magnetic transitions have been observed when gradually doping from ferromagnetic $CaCu_3Ge_4O_{12}$ to antiferromagnetic $CaCu_3Ti_4O_{12}$, and in turn to ferromagnetic $CaCu_3Sn_4O_{12}$, the mechanism of which is yet unknown but is apparently not due to bond angle-dependent superexchange interactions [7].

The structure of these materials provides important insight into, and restrictions on, the magnetic behavior of CCVO, where a magnetic transition (apparently antiferromagnetic) is seen at $T_N = 98$ K [1]. Both the $Co^{2+}$ and $V^{4+}$ ions in this cobaltovanadate are expected to be magnetic and Mott insulating, and seemingly carry a substantial orbital moment to account for the observed Curie-Weiss moment. The Co ion symmetry is *mmm* in the rectangular $CoO_4$ plaquettes that promote, as we will show, strong local anisotropy. Our calculations reveal that the Mott insulating character of the open-shell Co ion arises through the $d_{z^2}$ orbital in the local coordinate system. However, the overall cubic symmetry of the compound dictates that there are $CoO_4$ plaquettes perpendicular to each of the cubic axes, as can be seen in Fig. 1(a). The very narrow Co 3$d$ bands—very nearly localized orbitals—will promote strong magnetic anisotropy, with spin moment either perpendicular to, or within the plane of, the $O_4$ plaquette.

The $V^{4+}$ $d^1$ ion, with its $\bar{3}$ site symmetry, suggests a related conundrum. The four V ions have their individual symmetry axes along one of the four (111) directions. The occupied orbitals will be symmetry-adapted linear combinations of the $t_{2g}$ orbitals. Crystal field considerations suggest the $a_{1g}$ symmetric combination will lie *highest* in energy, leaving the doublet commonly denoted $e'_g$ singly occupied and therefore prime for orbital ordering. With the local (111) direction dictating the rotational symmetry, the $t_{2g}$ orbitals can be expressed in the form

$$\psi_m = \frac{1}{\sqrt{3}}\left(\zeta_m^0 d_{xy} + \zeta_m^1 d_{yz} + \zeta_m^2 d_{zx}\right), \quad (1)$$

 

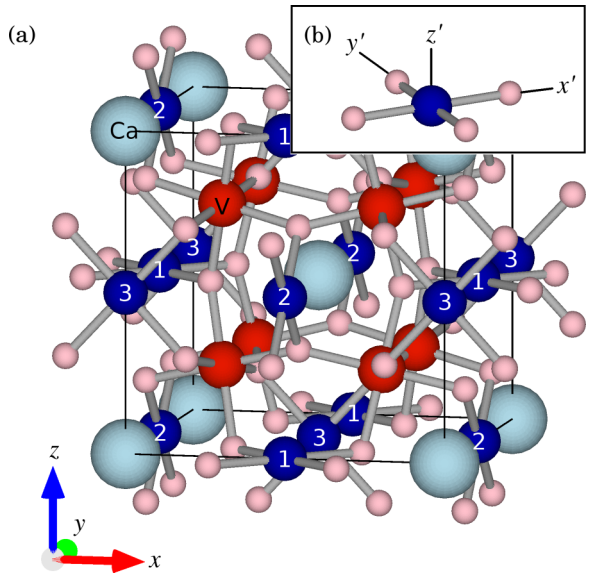


FIG. 1. (Color online) (a) Global coordinates and crystal structure of quadruple perovskite CCVO, containing two formula units per unit cell. The Co atoms (dark blue) are each surrounded by a plaquette of oxygens (pink), and the tilted $VO_6$ octahedra are nearly regular. The breaking of cubic symmetry due to spin-orbit coupling makes the three Co atoms (labeled 1 to 3) in the formula unit inequivalent. The magnetization quantization axis for our calculations, unless noted otherwise, is the $\hat{z}$ axis. To get the structure of fictitious compound $Ca_3CoV_4O_{12}$, replace Co atoms 1 and 2 with Ca. (b) Local coordinate system of a $CoO_4$ plaquette. Images were generated with VESTA [8].

where $\zeta_m = e^{2\pi mi/3}$ is the associated phase factor for threefold rotations. There is a vanishing orbital moment for the $a_{1g}$ member $m = 0$, but potentially large orbital moments for the $e'_g$ pair $m = \pm 1$. These orbital moments, hence the spin and net moments, should tend to lie along the (111) axis of symmetry of each V ion. Hence the V moments will be noncollinear among themselves, and also not collinear with the Co moments. In such a situation, interpretation of the magnetization data in the ordered state will become a challenging problem. We note that the noncollinearity that we are mentioning results from single-ion anisotropy rather than from competing, frustrated exchange coupling, which is beyond the scope of the present study.

CCVO is currently the only quadruple perovskite reported that has Co exclusively occupying the $A'$ site. Most known quadruple perovskites are half-metallic and semiconducting in the majority-spin channel; half-metallicity is often seen in perovskite oxides and other transition-metal oxides displaying CMR [9–11]. In this paper, we perform density functional studies on CCVO, and our methods indicate how CCVO becomes a Mott insulator. We also study a related fictitious system, $Ca_3CoV_4O_{12}$, in which two of CCVO's three Co atoms are replaced by Ca, so that spin and orbital effects may be better understood on a local scale.

## II. STRUCTURE OF CCVO AND CALCULATION METHODS

CCVO takes on a structure that can be pictured as a variant of the cubic perovskite oxide $ABO_3$. The superstructure $AA'_3B_4O_{12}$, with $Im\bar{3}$ space group, is formed by quadrupling the parent unit cell and replacing 3/4 of element $A$ with $A'$. Due to the introduction of $A'$, the symmetry of the structure is lowered by a large rotation of the $BO_6$ octahedra, which brings four oxygen ions closer to the $A'$ (Co) site to form a seemingly nearly square-planar environment, but we will show there is an important nonsquare component of the potential. Surprisingly, this particular quadruple perovskite houses $VO_6$ octahedra that are virtually regular: all V-O distances are identical, and the O-V-O angles deviate from 90° by only 0.04°. The natural local axes of course do not align with the global crystal axes. The $CoO_4$ plaquettes are not as regular, with the O-Co-O angles being 93.6° and 86.4°. Because the nonsquare aspect becomes important, we will refer to the unit as the $CoO_4$ plaquette.

Both Co and V ions are anticipated to be magnetic with Mott insulating character, so considerations of magnetic coupling arise. V ions lie on a simple cubic sublattice separated by $a/2 = 3.67$ Å, while Co ions lie on a bcc sublattice with the same nearest-neighbor Co-Co distance. The two perovskite $A$ and $B$ sublattices form a CsCl configuration, making it likely that nearest-neighbor Co-V exchange interactions (versus Co-Co or V-V) are the driving force for magnetic order.

In oxides, Co and V often display strongly correlated behavior, so orbitally independent treatments such as GGA and the local density approximation (LDA) do not provide the flexibility to handle a compound like CCVO. We have therefore employed the GGA + $U$ method [12,13], in which the intrashell Coulomb repulsion $U$ and interorbital Hund's $J$ magnetic couplings were applied to both Co and V with the following strengths: $U_{Co} = 5$ eV, $J_{Co} = 1$ eV, $U_V = 3.4$ eV, $J_V = 0.7$ eV. In studies of the effect of the value of $U$ in $Na_xCoO_2$ [14] and in $Sr_2CoO_4$ [15], it was found that once $U$ is larger than 3.5 eV, the results were relatively insensitive to $U$. For V, Korotin *et al.*, for example, used [16] $U_V = 3.6$ eV. Considering the observed semiconducting or small gap character of CCVO, with more screening than in wide-gap insulators, our values are modestly smaller than sometimes used but within the range of accepted values.

All-electron calculations of CCVO and C3CVO were done with the WIEN2K [17,18] program, which is based on a full-potential linearized augmented plane wave (FP-LAPW) method within the density functional theory formalism. The Perdew-Burke-Ernzerhof flavor [19] of the GGA was chosen for the exchange-correlation functional. We used a 17 × 17 × 17 $k$-point mesh for the cubic unit cell, outlined in Fig. 1(a). The sphere radii $R$ were set to 2.44, 2.04, 1.90, and 1.72 a.u. for Ca, Co, V, and O, respectively. $RK_{max} = 7.0$ was the cutoff for the plane-wave expansion of eigenstates. Because our intention here is to make contact as closely as possible with the electronic and magnetic behavior with available data, it is important to have correct interatomic distances to obtain bandwidths, etc., as accurately as possible. Thus we have used the experimental structural parameters throughout ($a = 7.3428$ Å, and measured internal coordinates) [1], rather than relaxing the structure. A collinear ferromagnetic (FM) configuration was adopted for this first study, to obtain insight into the intricate electronic and magnetic nature of CCVO. The likelihood of noncollinear ordering is discussed in the summary in Sec. IV.

The orbital moment on Co, and thus the magnetocrystalline anisotropy in CCVO, has been suggested to be large [1], reflecting the presence of strong spin-orbit coupling (SOC). It then is important to include SOC in the calculations. Without SOC, the symmetry of CCVO is cubic (even with spin polarization) so each of the three Co atoms in the stoichiometric formula is equivalent. Taking into account SOC, with the direction of magnetization **M** in any one of the three axial directions, lowers the symmetry, and the three Co ions in their individually oriented $CoO_4$ plaquettes are no longer equivalent, and we find very large differences in the orbital and even the spin moments. In this paper, the magnetization direction for all of our calculations will be along the $\hat{z}$ axis unless noted otherwise, and we will refer to the three different Co atoms as Co1, Co2, and Co3, labeled in Fig. 1(a) as 1, 2, and 3, respectively. The respective $CoO_4$ plaquettes are perpendicular to the $\hat{z}$, $\hat{x}$, and $\hat{y}$ directions, respectively.

Even with the addition of $U$, the orbital moment in Co perovskite oxides may be underestimated. In a fully relativistic treatment, there is an additional orbital correction, referred to as orbital polarization (OP) [20,21], which is an attractive energy that is proportional to the square of the orbital angular moment **L**. This OP correction has successfully been applied to intermetallics and especially to Co compounds that exhibit a large Co orbital moment [22–27]. The OP correction can be implemented in a phenomenological approach analogous to Hund's second rule that is implicit in GGA. Our results will show that orbital effects are indeed much larger within the OP scheme than within conventional GGA + $U$.

One the one hand, the symmetry lowering due to SOC raises questions about the character of magnetic ordering that occurs in CCVO. On the other hand, orbital moment formation and orientation seems to be a local phenomenon, almost dictating noncollinear magnetic order. To simplify some of the local questions, we have studied a theoretical cousin of CCVO, in which the Co2 and Co3 ions are replaced by simple $Ca^{2+}$, thereby isolating the Co1 ion for study. We present results for this model compound $Ca_3CoV_4O_{12}$, which we refer to as C3CVO, to demonstrate that the local environment by and large governs the magnetic character of the $CoO_4$ unit in CCVO.

## III. ELECTRONIC STRUCTURE ANALYSIS

### A. CCVO

The progression of the electronic and magnetic structure of FM CCVO with inclusion of $U$ and then SOC is displayed in the various panels of Fig. 2. The right-hand panels allow identification of the most relevant orbitals—those of the partially filled 3$d$ shell of Co. When SOC is included, the angular momentum basis orbitals $d_m$ are used for the projection, using the local coordinate system pictured in the Fig. 1 inset.

#### *1. Electronic structure within the GGA approach*

The collinear FM CCVO ground state within GGA is metallic, as revealed in the density of states (DOS) in Fig. 2(a). In all results to follow, occupation of the majority Co states is subject to only one uncertainty, namely whether all majority 3$d$ states are fully occupied or whether the $d_{x^2-y^2}$ orbitals, whose density lobes are directed toward the nearby $O^{2-}$ orbitals and thereby form the highest lying crystal field orbital, are occupied [high spin (HS)] or unoccupied [low spin (LS)]. The minority projected DOS (PDOS) shown in Fig. 2(d) allows identification of the crystal-field splittings of Co, since all

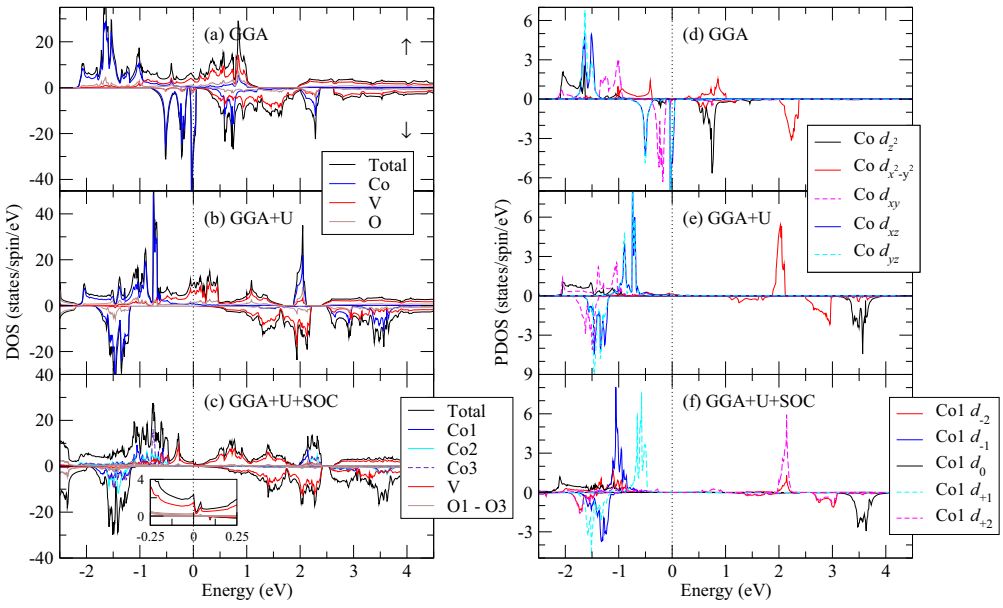


FIG. 2. (Color online) Spin-up and -down DOSs of CCVO, relative to the Fermi level $\varepsilon_F = 0$, resulting from FM alignment for (left panels) (a) GGA, (b) GGA + $U$, and (c) GGA + $U$ + SOC calculations, and (right panels) (d)–(f), the corresponding orbital- and spin-projected DOSs (in local coordinates) of Co. The top left (right) legend box applies to the two top left (right) graphs. The pseudogap mentioned in the text can be better seen in the blow-up of (c), inset in the bottom left panel. Ca does not contribute to the DOS within the featured range of energies. For the SOC-included calculations, the moment is along the $\hat{z}$ axis and the projected DOS plot is for Co1.

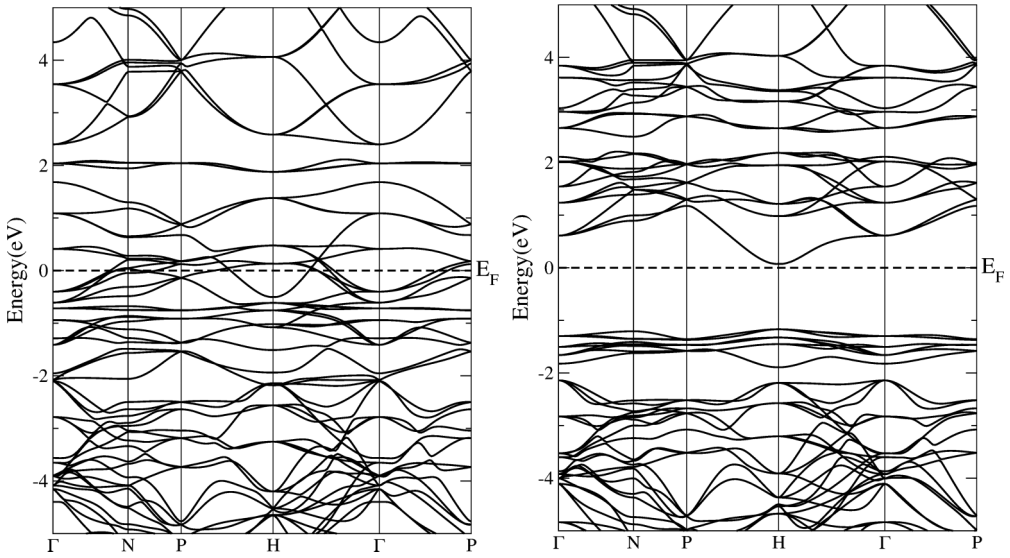


FIG. 3. Majority (left) and minority band structures resulting from a FM GGA + $U$ calculation of CCVO. The lack of a Mott insulating gap is due to V bands, as discussed in the text.

bands are narrow and peaks are evident. The crystal-field picture of Co site energies, relative to the mean energy, is as follows:

$$\begin{aligned} d_{x^2-y^2} &\quad 1.80\ \text{eV} \\ d_{z^2} &\quad 0.30\ \text{eV} \\ d_{yz} &\quad -0.45\ \text{eV} \\ d_{xy} &\quad -0.65\ \text{eV} \\ d_{xz} &\quad -0.95\ \text{eV} \end{aligned}$$

It was previously suggested [1], based on the bond valence method, that CCVO would have formal charges $Ca^{2+}$, $Co^{2+}$ $d^7$, $V^{4+}$ $d^1$, and $O^{2-}$. Our results are consistent with this assignment, which also is the only reasonable assignment consistent with integral values of formal charge. Within the GGA, the spectral density of the majority $d_{x^2-y^2}$ orbital [see Fig. 2(d)] is split above and below $\varepsilon_F$—i.e., an itinerant band. Although it is common for a transition metal ion's spin to be reduced by up to 20% by hybridization with oxygen, the spin moment of Co is reduced by 40%, to $1.77\mu_B$, from the HS value of $3\mu_B$; of course it is far too large for a LS value.

The majority V $t_{2g}$ bands extend from just below $\varepsilon_F$ to 1 eV. The V spin of $0.77\mu_B$ is consistent with a $d^1$ configuration; however, partial filling of the essentially localized minority Co $d_{xz}$ state suggests that some charge is taken from V. The very narrow Co minority $d_{yz}$,$d_{xy}$ states are filled. The localized $d_{yz}$ state with a very high density of states at $\varepsilon_F$, $N(\varepsilon_F)$, pins the Fermi level and implies, e.g., a charge-density wave or lattice instabilities. However, correlation effects and SOC have not been taken into account yet.

#### 2. *Electronic structure within the GGA+U approach*

Adding an on-site Coulomb repulsion on each of the Co and V ions results in a half-metallic electronic structure. The minority gap is 1.25 eV, the change evident in Figs. 2(a) and 2(b), and the corresponding GGA + $U$ band structure displayed in Fig. 3. Calculated moments are tabulated in Table I. One effect of $U$ has been to remove all Co states from near the Fermi level, leaving the clear $Co^{2+}$ formal charge with $d_{x^2-y^2}$ of both spins and minority $d_{z^2}$ unoccupied. With four majority and three minority electrons on Co, $U$ has driven Co through a spin-state transition, from roughly HS to clearly LS, with moment $1.0\mu_B$, as is common for square-planar geometry. The Co ion is Mott insulating in character.

Plotted in Figs. 2(d) and 2(e) are the PDOSs of Co in CCVO from GGA and GGA + $U$ calculations, respectively. If the $O_4$ plaquette around Co were perfectly regular, the $d_{xz}$ and $d_{yz}$ states would be degenerate. Applying $U_{Co}$ lowers the sharp $d_{xz}$ and $d_{yz}$ peaks in the minority channel, initially centered at $\varepsilon_F$, to 1.5 eV below $\varepsilon_F$. The $d_{z^2}$ orbital is affected most by $U_{Co}$, the minority state being displaced higher in energy by almost 3 eV. In the majority channel, most of the states are shifted up; the formerly divided $d_{x^2-y^2}$ states have coalesced to comprise the single hole in the majority channel.

Vanadium, on the other hand, drives the half-metallic nature by declining to open a Mott gap, retaining a majority band crossing $\varepsilon_F$ with $N(\varepsilon_F) = 6.1\ \text{eV}^{-1}$ $\text{spin}^{-1}$. However,

TABLE I. Spin and orbital moments of the Co and V ions in CCVO, obtained from GGA, GGA + $U$, and GGA + $U$ + SOC calculations, as well as moments in C3CVO obtained from a GGA + $U$ + SOC calculation. Moment are given in $\mu_B$.

| | | | $\mu_{spin}$ | $\mu_{orb}$ |
|---|---|---|---|---|
| CCVO | GGA | Co | 1.77 | |
| | | V | 0.79 | |
| | | Co1–Co3 | 1.00 | |
| | GGA + $U$ | V | 0.87 | |
| | GGA + $U$ + SOC | Co1 | 0.94 | −0.75 |
| | | Co2 | 0.93 | −0.05 |
| | | Co3 | 0.93 | +0.07 |
| | | V | 0.84 | −0.36 |
| C3CVO | GGA + $U$ + SOC | Co | 0.97 | −0.08 |
| | | V | 0.75 | −0.07 |

the symmetry used up to this point retains the nearly cubic local symmetry of V and more specifically the $e_g'$ degeneracy; symmetry-breaking of some kind is required to break this symmetry and allow a Mott insulating V configuration. However, SOC has not yet been taken into account and its effect is crucial.

#### 3. Electronic structure from GGA+U+SOC

Incorporating SOC lowers the symmetry, one outcome being that the Co ions become inequivalent. Unexpected behavior was encountered at the GGA+SOC level when directing the spin along the (say) $\hat{z}$ axis: the three Co ions developed strong differences, violating the observed cubic symmetry (although the differences might be difficult to see in standard x-ray diffraction). Due to the very narrow Co $3d$ bands near or at the Fermi level, self-consistency became difficult and the behavior was suggestive of multiple local minima with similar energies.

Related computational (mis)behavior arises even when lowering the symmetry by adding SOC *after* GGA + $U$, when (our subsequent results show) all Co states are in the process of being removed from the Fermi level. Large orbitals moments arise, which is surprising at first glance because $d_{+1}, d_{-1}$, or $d_{+2}, d_{-2}$ occupations (relative to the spin direction) must become unbalanced while their real and imaginary parts are nondegenerate and thus are not so readily mixed. This choice of order in including $U$ and SOC results in antiferromagnetic (AFM) tendencies—the spin of one of the three Co atoms reverses direction, and orbital moments are vastly differing.

To control the behavior of the Co moments, we devised the following procedure. Before adding $U$ or SOC, the symmetry was broken (for example, by displacing an atom by a physically negligible amount), which allowed the calculation to proceed from the GGA solution rather than to begin anew. In addition, we enforced a total fixed spin moment (FSM) equal to that obtained from a calculation before the symmetry breaking; otherwise, the artificial symmetry-breaking again makes self-consistency difficult. With the total moment fixed, the electronic and magnetic structures were relaxed. Then with the moment freed, $U$ was added and taken to self-consistency, and finally SOC was incorporated. The order of these last two steps was found to be important. Carried out in this way, the unrealistically large differences between the Co ions was lessened. All results in this paper of GGA + $U$ + SOC calculations for CCVO were obtained from this "infinitesimal broken symmetry+initial FSM" protocol. We mention in passing that, since the experimental evidence suggested AFM order (at least not ferromagnetic order), we attempted some AFM calculations, which require further doubling of the unit cell. These calculations encountered additional difficulties, including resulting in considerably differing Co spins. We did not succeed in finding a procedure to avoid this in the AFM case, and we discuss in the final section why doing so might not be any more realistic than the FM ordered results that we present.

Including SOC dramatically changes the V-derived majority DOS at and around the Fermi energy, as shown in Fig. 2(c). At the value of $U_V$ that we have chosen (3.4 eV), the V manifold centered at $\varepsilon_F$ opens, leaving a pseudogap. With our chosen values of $U$, this result leaves CCVO as a half-semimetal with a slight band overlap in the majority channel; a somewhat larger value of $U_V$ results in a FM Mott insulator state. The minority spin spectrum, on the other hand, changes very little. The gap is a result of relativity—accounting for SOC—which breaks the degeneracy of the V $d_{\pm1}$ orbitals and creates a substantial orbital moment of $-0.36\mu_B$ that cancels 40% of the spin moment. Despite the significant changes to the V ion when SOC is included, the formal valence remains unchanged.

Though the changes to the Co1 spectrum in Fig. 2(f) seem less important, they are such to drive an orbital moment of $0.75\mu_B$ on the Co1 ion. The unoccupied minority $d_{z^2}$ orbital becomes the $d_0$ peak and contributes nothing to the orbital moment. The unoccupied majority $d_{x^2-y^2}$ orbital becomes about 85% $d_{+2}$ and 15% $d_{-2}$, thus providing the net orbital moment. This effect is enhanced (perhaps, one might say, enabled) by the nonsquare symmetry of the $CoO_4$ unit.

TABLE II. Spin and orbital moments of Co1, Co2, Co3, and V in CCVO, and Co and V for each $\hat{z}$, $\hat{y}$, and $\hat{x}$ magnetization direction in fictitious C3CVO, all from GGA+OP+SOC calculations. Units are in $\mu_B$ and magnetization directions are in parentheses next to the atom.

| | | $\mu_{spin}$ | $\mu_{orb}$ |
|---|---|---|---|
| | Co1 ($\hat{z}$) | 1.69 | 0.25 |
| CCVO | Co2 ($\hat{z}$) | 1.83 | 0.87 |
| | Co3 ($\hat{z}$) | 2.05 | 1.54 |
| | V ($\hat{z}$) | 0.75 | −0.02 |
| | Co ($\hat{z}$) | 1.52 | 0.27 |
| C3CVO | Co ($\hat{y}$) | 1.51 | 0.43 |
| | Co ($\hat{x}$) | 1.77 | 1.11 |
| | V ($\hat{x},\hat{y},\hat{z}$) | 0.71–0.73 | −0.01 |

#### 4. Beyond GGA+U+SOC

A fully relativistic treatment of the electronic structure reveals an orbital polarization (OP) energy and associated potential analogous to that of spin polarization. The OP method developed by Brooks [20] and by Eriksson *et al.* [21] is an orbitally dependent correction to energy functionals such as GGA and LDA. Hund's second rule is not taken into account in these functionals, leading to an underestimation of the orbital moment of many $d$ metals [28]. OP adds to the energy functional a correlation energy functional modeled as

$$E_{OP} = -\frac{1}{2}\sum_{\sigma} B_\sigma L_\sigma^2,$$

which acts to energetically favor larger orbital moments, while the resulting potential makes $m_\ell$-dependent shifts in bands. Here, $B = F_2 - 5F_4$ is the Racah parameter in terms of the Slater integrals $F_2$ and $F_4$, $L$ is the orbital moment in units of $\mu_B$, and $\sigma$ denotes spin. For Co, $B = 0.079$ eV; for V, 0.071 eV. The spin dependence (<1%) of these parameters is included but is unimportant.

The moments from the OP method (GGA+OP+SOC) are listed at the top of Table II. The largest Co orbital moment in the OP scheme is $1.5\mu_B$, more than double the value obtained from the GGA + $U$ + SOC calculation. However, this time it is Co3, whose $O_4$ plaquette is perpendicular to $\hat{y}$, that possesses

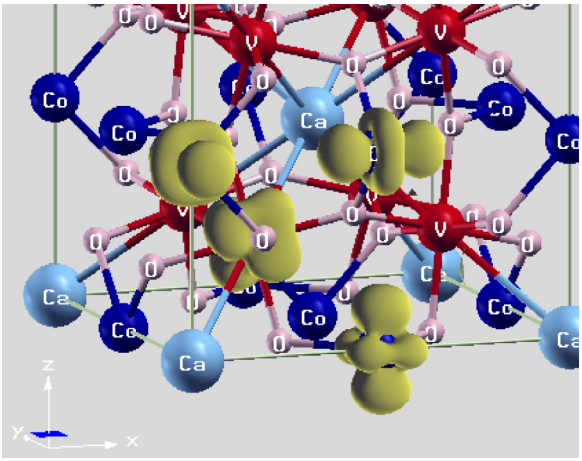


FIG. 4. (Color online) Spin-density isosurface of the valence state of CCVO obtained from a GGA + $U$ + SOC calculation. The V isosurface is the central one. Differences of the Co spin densities are discussed in the text.

the large moment; the spin and orbital moments lie with the $CoO_4$ plane rather than perpendicular to it. Co2 also has a large orbital moment, $0.9\mu_B$, again lying with the plane of the $CoO_4$ unit. The three Co spin moments range from 1.7 to $2.0\mu_B$; these more nearly HS values are (almost) twice the size of the LS moments from the GGA + $U$ + SOC method. Thus OP enhances orbital moments but, unexpectedly, feeds back to enhance greatly the spin moments while complicating the atomic configurations of the Co ions.

The three-dimensional isosurface of the GGA + $U$ + SOC valence spin density of CCVO is provided in Fig. 4. The spin isosurfaces centered on each of the three cobalts take roughly a $d_{z^2}$-orbital shape, due to the Mott-Hubbard spitting of the Co $d_{z^2}$ orbitals. They do not align collinearly but along each $O_4$ plaquette's normal axis. The three show certain differences; the "ring" around the Co1 atom, when compared to that of Co2 and Co3, is more squarelike, some $d_{x^2-y^2}$-like character in addition to the stronger $d_{z^2}$ character. This difference in spin density is a consequence of SOC—without it, all three Co isosurfaces would be identical—and its magnetization direction with respect to the direction of the $O_4$ plaquette.

The spin isosurface around V, shown also in Fig. 4, is essentially identical to its total valence *charge*-density isosurface, since the occupied V 3$d$ states originate from the majority channel only. These V $d$ states are concentrated between −0.45 eV and the Fermi energy, and they feature lobes corresponding to the linear combination in Eq. (1) and maintaining $\bar{3}$ symmetry along the local (111) symmetry axis.

#### 5. Discussion of results for CCVO

Inclusion of SOC, and more so with GGA+OP+SOC, indicates the likelihood of very large Co orbital moments, as suggested by Ovsyannikov *et al.* from analysis of the susceptibility [1]. Furthermore, the extreme narrowness of the Co bands suggest that the physics is local: the magnetic anisotropy is determined by the $CoO_4$ configuration. The perpendicular axis (the local $\hat{z}$ axis) seems the natural direction for a large orbital moment, and thus the spin as well. While GGA + $U$ + SOC gave that result, including OP shows that large orbital moments may well lie within the plane of the $CoO_4$ unit. In any case, if the physics is local and each unit behaves the same, the Co moments will be noncollinear. Similarly, the natural axis for the V orbital moment is along its (111) symmetry direction, a different direction for each V ion.

The strong indications are that the magnetic order is noncollinear, possibly reinforced by competing exchange interaction and suffering canting tendencies due to the Dzyaloshinskii-Moriya interaction between Co-V and V-V pairs. This combination of strong correlation, important spin-orbit coupling in which the orbital moments feed back on the spin density, and an intricate geometrical arrangement presents a daunting challenge for an *ab initio* calculation. With substantial orbital moments, the magnetic coupling between total moments becomes tensorial rather than scalar. Treating and understanding the coupling would be a challenge even if the exchange tensors were known, and it has recently been shown that obtaining this tensor coupling when SOC coupling has large effects requires special technology [29].

CCVO's effective paramagnetic moment $\mu_{\text{eff}}$ derived from magnetic susceptibility measurements [1] is $9.3\mu_B$. Assuming the $S = \frac{1}{2}$ moment on $V^{4+}$, the effective net moment of Co is $4.4\mu_B$, implying a considerable orbital moment of Co up to $\sim 2.5\mu_B$, depending on the Co spin moment. Only recently have unusually large orbital moments for Co in perovskites been reported, yet not exceeding $1.8\mu_B$. The possibility that V also has a moment does not help to account for the observed value, since by Hund's rules it would cancel the spin moment, as shown in Table I.

We do observe a large orbital moment of $0.7\mu_B$ on Co1 in the GGA + $U$ + SOC result, but *antiparallel* to the spin. The other two cobalts have small, typically sized orbital moments. For the (001) spin direction, we have presumed that Co1 is the distinctive Co, since its $O_4$ plaquette is the one that is perpendicular to the magnetization quantization axis, and its large moment lies along that axis. Orbital polarization, analogous to spin polarization (Hund's rule), has been found to improve calculated orbital moments in several magnetic materials, and it produces large orbital moments for CCVO. While $0.7\mu_B$ is an impressive value for a 3$d$ orbital moment, OP more than doubles this to $1.5\mu_B$. The unique Co in the GGA+OP+SOC scheme is Co3, however, not Co1, such that the large orbital moment lies parallel to the $O_4$ plaquette.

### B. C3CVO

Continuing with the theme that the $CoO_4$ behavior involved primarily local physics, we chose to adopt a simpler model that contains only one Co ion. Two of the $Co^{2+}$ ions are replaced with $Ca^{2+}$ ions, greatly simplifying both the conceptual issues and the self-consistency process. We proceed to investigate some of the behavior of this model compound $Ca_3CoV_4O_{12}$ (C3CVO).

#### 1. GGA+U+SOC

We have set the magnetization direction for C3CVO to be perpendicular to the $O_4$ plane on which the remaining Co lies; this is equivalent to keeping Co1, and replacing Co2 and Co3

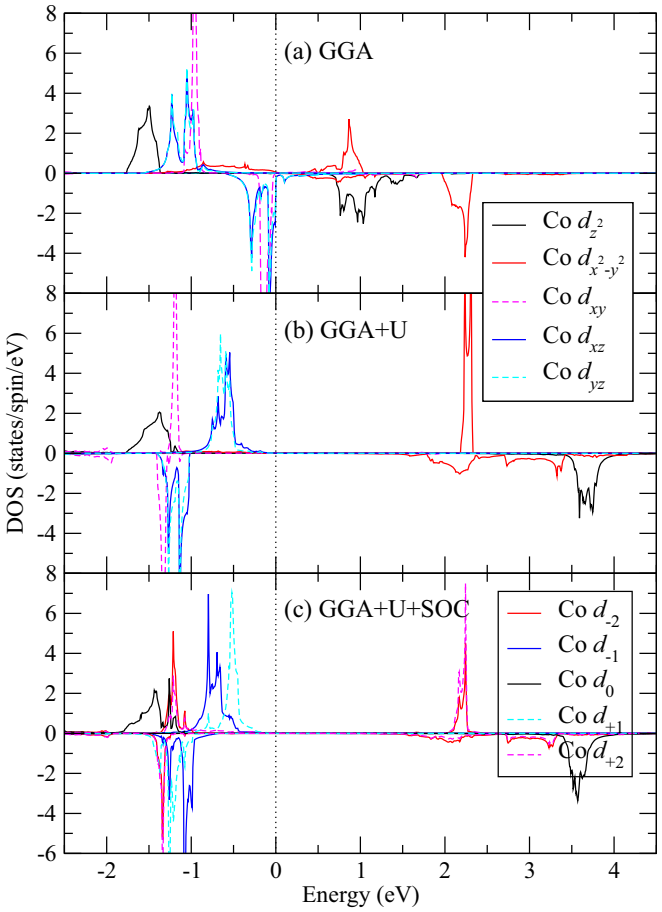


FIG. 5. (Color online) Spin-up and -down, orbitally projected PDOSs of Co in CCVO resulting from FM alignment using (a) GGA, (b) GGA + $U$, and (c) GGA + $U$ + SOC(001) calculations. The top legend box applies to the top two graphs.

with Ca in Fig. 1(a). Comparing the PDOS in Fig. 5 for C3CVO to the right-hand panels of Fig. 2 for CCVO, it is apparent that the electronic environment of Co in C3CVO is similar to that of Co1 in CCVO when SOC is included. This confirms that C3CVO represents reasonably the local planar environment of Co1 in CCVO without the complications from the other Co ions. The general characteristics of GGA, $U$, and SOC produced in C3CVO are very much like those seen in CCVO. With the GGA + $U$ + SOC method, C3CVO, like CCVO, remains metallic in the majority channel and semimetallic in the minority. A pseudogap (near Mott insulating) feature made up of V states at the Fermi energy (not shown), similar to that in CCVO, is also present in C3CVO.

Unexpectedly, the orbital moments of V and Co in C3CVO are much smaller than those of V and analogous Co1 in CCVO, as displayed at the bottom of Table I. In C3CVO, the orbital moment of V of 0.07$\mu_B$ is only one-fifth of its value in CCVO. We note that we have not oriented the spin along a (111) direction, where the V orbital moment may be larger. The difference in the Co orbital moment is even larger, with C3CVO's Co moment (0.08$\mu_B$) having only 10% of the strength that it has in CCVO (0.75$\mu_B$), due perhaps to the absence of the Co-V network of exchange.

### 2. *GGA+OP+SOC*

Referring back to Fig. 1(a), when CCVO's quantization axis is the $\hat{z}$ axis, Co1 is analogous to the sole Co in C3CVO when *its* quantization axis is also the $\hat{z}$ axis. Similarly, Co2 (Co3) is analogous to the only Co in C3CVO when quantization is in the $\hat{y}$ ($\hat{x}$) direction. The analogies are reflected by the ordering of the entries in Table II. The trends in CCVO and C3CVO are common, both in spin and orbital moments, which increase from Co1 to Co2 to Co3, and also as the magnetization axis is rotated in C3CVO from $\hat{z}$ to $\hat{y}$ to $\hat{x}$. In the GGA + $U$ + SOC scheme, the difference between the orbital moment of Co1 in CCVO and that of Co in C3CVO was tenfold. OP, however, lessens this difference: the largest orbital moment of Co in C3CVO is 1.1$\mu_B$, which is 75% of the maximum orbital moment of 1.5$\mu_B$ in the full structure of CCVO. This difference arises from the differences in Co 3$d$ occupation.

Co in C3CVO has the largest orbital moment when $\mathbf{M} \parallel \hat{x}$, with an analogous result in CCVO—i.e., Co3 has the largest $\mu_{orb}$. The uniqueness of Co3 in the OP+SOC method is curious, since it is the Co1 plaquette that is perpendicular to the quantization axis. The strong coupling of the size of $\mu_{orb}$ to the local spin direction can be understood by studying the Co DOSs presented in Fig. 6. In Fig. 6(a), the three Co DOSs are compared in one plot. Panels (b), (c), and (d) below it are the Co states of C3CVO with quantization in the various

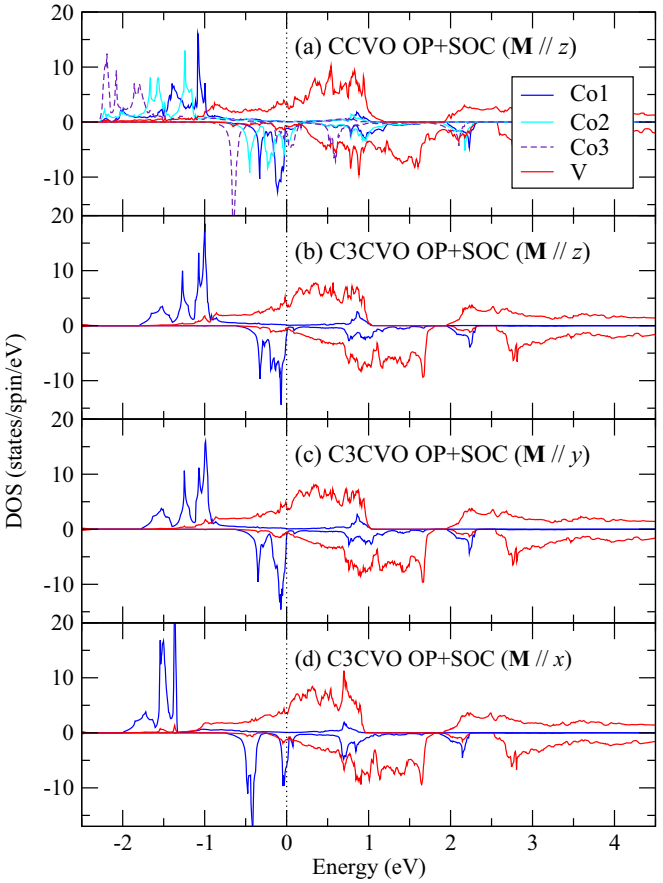


FIG. 6. (Color online) GGA+OP+SOC DOSs of (a) Co sites and V site in CCVO, and (b)–(d) Co and V sites in C3CVO. **M** is parallel to $\hat{z}$ in (a) and (b), to $\hat{y}$ in (c), and to $\hat{x}$ in (d).

orientations, and it is clear that the DOSs are similar when $\mathbf{M} \parallel \hat{z}$ and $\mathbf{M} \parallel \hat{y}$ while different when $\mathbf{M} \parallel \hat{x}$. The spin-up occupied Co states are lower in energy when $\mathbf{M} \parallel \hat{x}$, and the down-spin occupied peak, instead of butting up against the edge of the Fermi level, has states that pass above $\varepsilon_F$. These additional unoccupied states provide the distinction between $\mathbf{M} \parallel \hat{x}$ and $\mathbf{M}$ along the other two axial directions. The orbital potential evidently produces important shifts in positions of Co 3*d* bands.

In Fig. 6, providing the PDOSs of CCVO and C3CVO for the OP+SOC results, one can observe that the Co1 electronic states in CCVO in panel (a) are very similar to those of C3CVO in (b) and (c). Meanwhile, Co3 of CCVO, like Co of C3CVO in Fig. 6(d) ($\mathbf{M} \parallel \hat{x}$), has more strongly bound majority occupied states, and unoccupied states "leak" out of the minority peak centered just below $\varepsilon_F$. Co2 in CCVO and Co in C3CVO when $\mathbf{M} \parallel \hat{y}$ do not share as many similarities as the other two analogous pairs, and that is reflected in the differing spin and orbital values in Table II.

## IV. DISCUSSION AND SUMMARY

Our numerous investigations into the electronic and magnetic structure of CCVO reveal a great deal of complexity, even considering the three Co and four V ions in the primitive cell, each with its own natural axis of exact (V) or approximate (Co) symmetry. This complexity is the result of (i) two types of open-shell cations, (ii) strong correlation in narrow bands, (iii) important and in some cases dominating spin-orbit coupling, and (iv) an intricate three-dimensional network. To account for the insulating nature, both Co and V must display Mott insulating character. While the crystal-field splittings on the Co site—a span of 2.75 eV—are typical for a 3*d* ion in an oxide, the subsplittings become very important given the very narrow Co 3*d* bands. Though these bands are narrow and separate above and below the Fermi level, the Co spin is not very representative of either the HS or LS state, a reflection of some charge-transfer character of this cobaltovanadate. The $O_4$ plaquette has an important nonsquare component of the potential, so spin that is directed in the $\hat{x}$ and $\hat{y}$ directions produces very different orbital moments.

We have not given sufficient attention to the V ion. Each of the V ions has its own threefold axis (symmetry related, of course), which provides a natural axis for the orbital moment, and hence the spin moment. The $d^1$ configuration in the $e'_g$ doublet requires SOC, orbital ordering, or structural distortion to provide the splitting necessary for a Mott gap.

In addition to the widely applied GGA + *U* + SOC method, we have explored the application of the little used orbital polarization potential via GGA+OP+SOC. This OP is an analog of the spin-polarization potential within GGA but is roughly an order of magnitude smaller, but it arises in a fully relativistic theory of electronic structure and should be applied more widely and studied. Both methods give a tendency toward very large orbital moments, but the behavior is different in the two approaches.

Whichever approach is used, only one of the three Co ions acquires a large $\mu_{orb}$ when the spin moments (hence orbital moments) are restricted to be collinear. This observation, together with the large orbital moment inferred from experiment and the fact that the mechanisms of magnetization appear to be local, suggests that the Co moments will be noncollinear, each directed along its own large $\mu_{orb}$ axis. Analogously, the V moments are likely to be noncollinear as well, and in different directions [(111) axes] than the Co moments.

$CaCo_3V_4O_{12}$ thus presents a very challenging electronic and magnetic structure problem. After starting from the GGA starting point, both the Hubbard *U* and spin-orbit coupling—together with the required great reduction in symmetry—are required to produce the observed Mott insulating state. As we have mentioned, a correct calculation also includes the orbital polarization term, one whose evident effect (from its form of the energy) is to enhance the orbital moment. However, the resulting orbital-dependent potential shifts bands, and the final outcome can be more complicated than a simple enhancement. Finally, all moments (spin plus orbital) should be treated noncollinearly. A calculation of this type—noncollinear GGA + *U* + OP + SOC—might be the first of its kind.

## ACKNOWLEDGMENTS

We acknowledge many cogent observations from A. S. Botana throughout the course of this study, and we thank V. Pardo for many discussions on the impact of spin-orbit coupling and the origin of orbital moments. This research was supported by U.S. Department of Energy Grant No. DE-FG02-04ER46111.

[1] S. V. Ovsyannikov, Y. G. Zainulin, N. I. Kadyrova, A. P. Tyutyunnik, A. S. Semenova, D. Kasinathan, A. A. Tsirlin, N. Miyajima, and A. E. Karkin, Inorg. Chem. **52**, 11703 (2013).

[2] Z. Zeng, M. Greenblatt, M. A. Subramanian, and M. Croft, Phys. Rev. Lett. **82**, 3164 (1999).

[3] K. Takata, I. Yamada, M. Azuma, M. Takano, and Y. Shimakawa, Phys. Rev. B **76**, 024429 (2007).

[4] J. A. Alonso, J. Snchez-Bentez, A. De Andrs, M. J. Martnez-Lope, M. T. Casais, and J. L. Martnez, Appl. Phys. Lett. **83**, 2623 (2003).

[5] M. Subramanian, D. Li, N. Duan, B. Reisner, and A. Sleight, J. Solid State Chem. **151**, 323 (2000).

[6] Y. Lin, Y. B. Chen, T. Garret, S. W. Liu, C. L. Chen, L. Chen, R. P. Bontchev, A. Jacobson, J. C. Jiang, E. I. Meletis *et al.*, Appl. Phys. Lett. **81**, 631 (2002).

[7] Y. Shimakawa, H. Shiraki, and T. Saito, J. Phys. Soc. Jpn. **77**, 113702 (2008).

[8] K. Momma and F. Izumi, J. Appl. Crystallogr. **44**, 1272 (2011).

[9] S. J. Youn and B. I. Min, Phys. Rev. B **56**, 12046 (1997).

[10] A. K.-I. Kob, T. Kimura, H. Sawada, K. Terakura, and Y. Tokura, Nature (London) **395**, 677 (1998).

[11] J.-H. Park, S.-W. Cheong, and C. T. Chen, Phys. Rev. B **55**, 11072 (1997).

[12] V. I. Anisimov, J. Zaanen, and O. K. Andersen, Phys. Rev. B **44**, 943 (1991).
[13] E. R. Ylvisaker, W. E. Pickett, and K. Koepernik, Phys. Rev. B **79**, 035103 (2009).
[14] K.-W. Lee, J. Kuneš, P. Novak, and W. E. Pickett, Phys. Rev. Lett. **94**, 026403 (2005).
[15] K.-W. Lee and W. E. Pickett, Phys. Rev. B **73**, 174428 (2006).
[16] M. A. Korotin, I. S. Elfimov, V. I. Anisimov, M. Troyer, and D. I. Khomskii, Phys. Rev. Lett. **83**, 1387 (1999).
[17] P. Blaha, K. Schwarz, P. Sorantin, and S. Trickey, Comput. Phys. Commun. **59**, 399 (1990).
[18] K. Schwarz and P. Blaha, Comput. Mater. Sci. **28**, 259 (2003).
[19] J. P. Perdew, K. Burke, and M. Ernzerhof, Phys. Rev. Lett. **77**, 3865 (1996).
[20] M. Brooks, Physica B+C **130**, 6 (1985).
[21] O. Eriksson, B. Johansson, R. C. Albers, A. M. Boring, and M. S. S. Brooks, Phys. Rev. B **42**, 2707 (1990).
[22] Y. Wu, J. Stöhr, B. D. Hermsmeier, M. G. Samant, and D. Weller, Phys. Rev. Lett. **69**, 2307 (1992).
[23] J. Trygg, B. Johansson, O. Eriksson, and J. M. Wills, Phys. Rev. Lett. **75**, 2871 (1995).
[24] M. Sargolzaei, M. Richter, K. Koepernik, I. Opahle, H. Eschrig, and I. Chaplygin, Phys. Rev. B **74**, 224410 (2006).
[25] S. Wurmehl, G. H. Fecher, K. Kroth, F. Kronast, H. A. Drr, Y. Takeda, Y. Saitoh, K. Kobayashi, H.-J. Lin, G. Schnhense *et al.*, J. Phys. D **39**, 803 (2006).
[26] A. Saúl, D. Vodenicarevic, and G. Radtke, Phys. Rev. B **87**, 024403 (2013).
[27] N. Hollmann, S. Agrestini, Z. Hu, Z. He, M. Schmidt, C.-Y. Kuo, M. Rotter, A. A. Nugroho, V. Sessi, A. Tanaka *et al.*, Phys. Rev. B **89**, 201101 (2014).
[28] G. H. O. Daalderop, P. J. Kelly, and M. F. H. Schuurmans, Phys. Rev. B **44**, 12054 (1991).
[29] S.-T. Pi, R. Nanguneri, and S. Savrasov, Phys. Rev. Lett. **112**, 077203 (2014).